Electronic Supplementary Material (ESI) for Journal of Materials Chemistry C.

Supporting Information

Controlling ions and electrons in aqueous solution: an alternative point of view of the charge-transport behavior of eumelanin-inspired material

João V. Paulin, Mariane P. Pereira, Bruna A. Bregadiolli, João P. Cachaneski-Lopes, Carlos F.O. Graeff, Augusto Batagin-Neto, and Carlos C.B. Bufon**

A) Additional experimental data analysis.

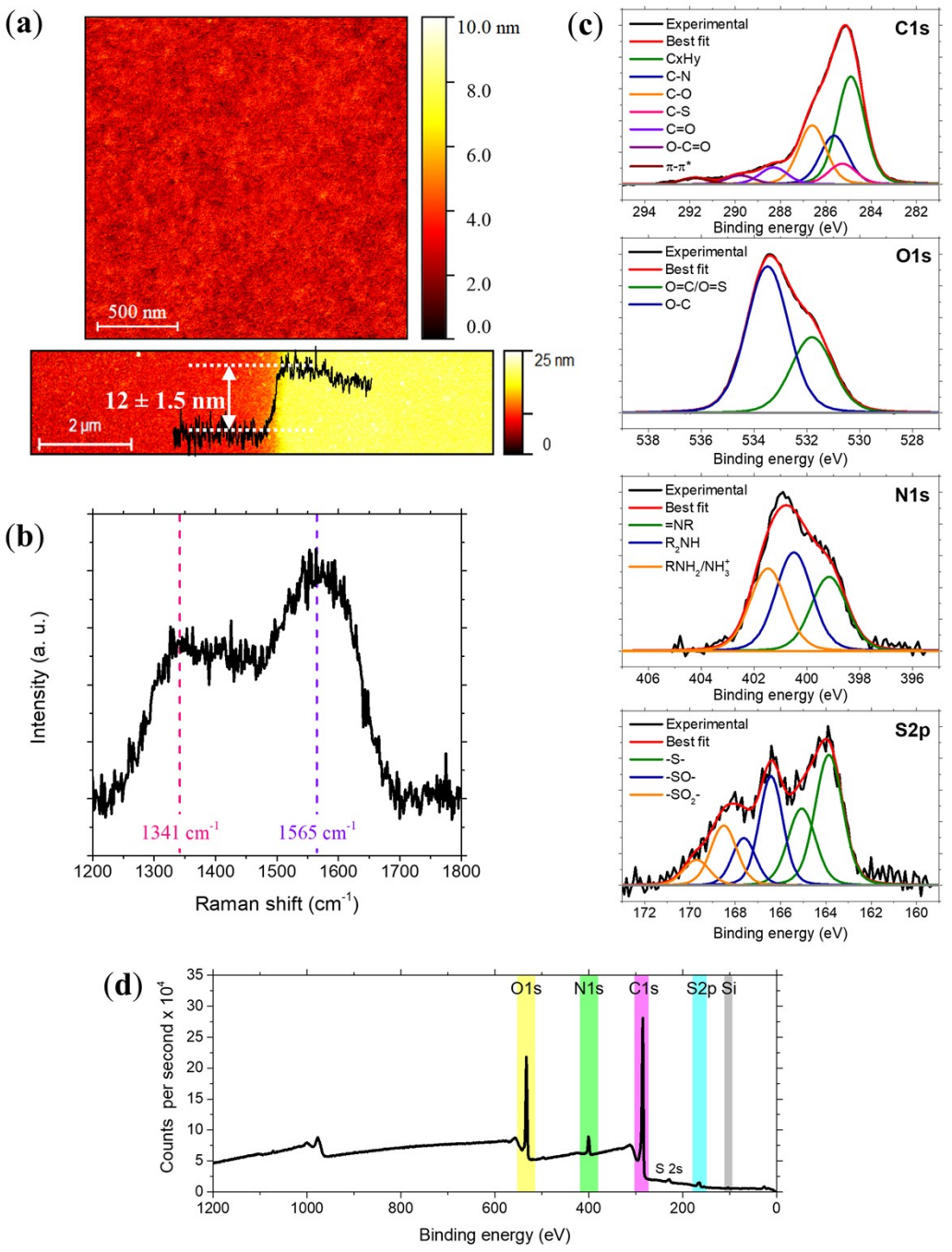

Figure S1. Characteristics of SMel thin-films in a glass substrate. (a) AFM topography (2 μm × 2 μm) image and profile (*10* µm × 2 μm) thickness. (b) Raman spectra. (c) C1s, O1s, N1s, and S2p high-resolution XPS spectra with their respective simulation analysis. $S2p_{3/2}$ refers to high intensity

and low binding energy, whereas $S2p_{1/2}$ to the opposite behavior. (d) XPS wide-scan survey spectrum.

Table S1. C1s, O1s, N1s, and S2p photoelectron binding energies assignments and atomic composition (%at) of SMel films.

Region	Functionality	Binding energy (± 0.2 eV)	Atomic composition (% at)
C1s	CxHy	284.9	40.4
	C-S	285.3	7.7
	C-N	285.6	18.2
	C-O	286.6	22.0
	C=O	288.3	6.3
	O-C=O	289.8	3.2
	π-π*	291.8	2.3
N1s	=NR	399.2	29.0
	R_2NH	400.5	38.7
	RNH_2/NH_3^+	401.5	32.3
O1s	O=C/O=S	531.8	34.1
	O-C	533.5	65.9
$S2p_{3/2}$	-S-	163.9	31.0
	-SO-	166.4	22.2
	$-SO_2-$	168.5	13.4
$S2p_{1/2}$	-S-	165.1	18.1
	-SO-	167.3	9.7
	$-SO_2-$	169.7	5.6

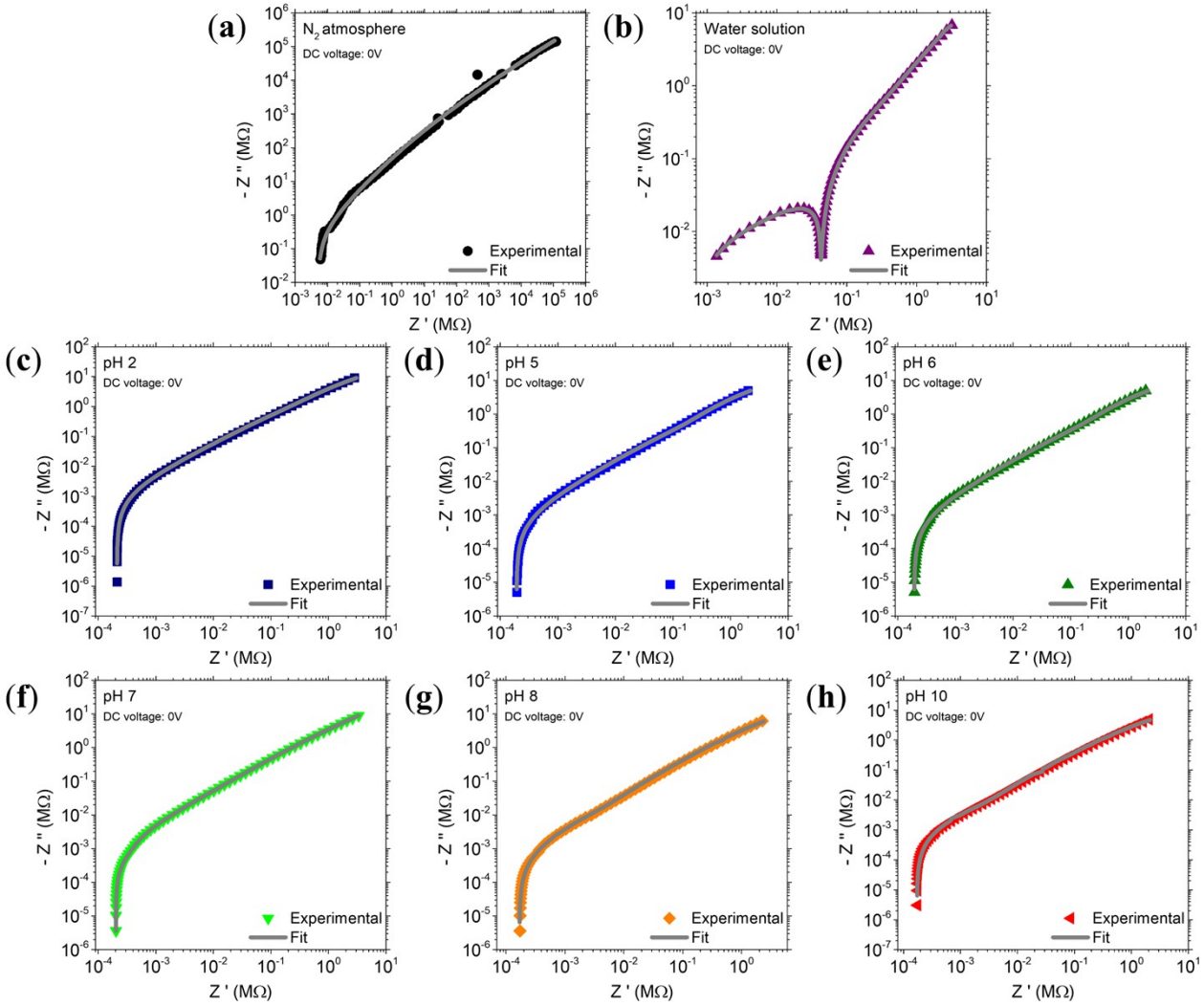

Figure S2. EIS fitting of SMel coated IDE at an offset DC voltage of 0V in different ambient conditions. The graphs are on a log-log scale showing low and high-frequency regimes.

Table S2: Fitting parameters of the humidity data according to the Randles equivalent circuit at zero DC voltage. The Warburg diffusion element is divided into three components: W-R represents diffusion impedance, W-T is system diffusion time, and W-P is an exponential factor.

Element	N_2	Water	pH 2	pH 5	pH 6	pH 7	pH 8	pH 10
R_1 (Ω)	4996.00	818.80	211.90	191.60	169.30	201.60	169.10	172.30
Q_1 (Ω^{-1})	3.63×10^{-12}	3.41×10^{-11}	1.72×10^{-6}	1.35×10^{-6}	5.17×10^{-5}	1.17×10^{-6}	1.06×10^{-6}	7.08×10^{-7}
η_1 (unitless)	0.99	1.00	0.84	0.85	0.62	0.88	1.00	0.95
R_2 (Ω)	4.02×10^{4}	4.13×10^{4}	1.51×10^{5}	9.05×10^{4}	3.50×10^{6}	3.09×10^{5}	1.15×10^{3}	1.33×10^{2}
W-R (Ω)	8.09×10^{11}	4.51×10^{7}	0.18	45.25	8.07	1.75×10^{4}	1.73×10^{4}	6.00×10^{4}
W-T	27.53	18.51	8.99	8.98	0.05	8.97	8.97	8.94
W-P	0.38	0.74	1.00	1.00	1.00	1.00	1.00	1.00
Q_2 (Ω^{-1})	-	9.26×10^{-7}	1.55×10^{-7}	2.61×10^{-7}	6.39×10^{-7}	1.53×10^{-7}	2.18×10^{-7}	2.67×10^{-7}
η_2 (unitless)	-	0.95	0.90	0.86	0.76	0.89	0.86	0.85
R_3 (Ω)	-	6.81×10^{4}	5.77×10^{7}	2.78×10^{7}	1.62×10^{7}	5.35×10^{7}	4.16×10^{7}	2.77×10^{7}
χ^2	0.112	0.000	0.002	0.004	0.014	0.004	0.006	0.005

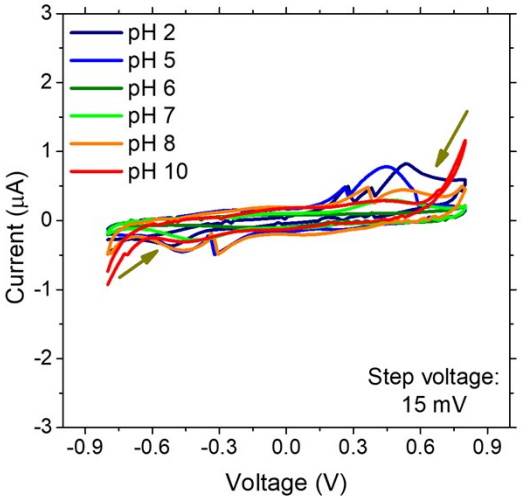

Figure S3. I-V curves of PBS electrolyte at different pH: (a) pH 2, (b) pH 5, (c) pH 6, (d) pH 7, (e) pH 8, and (f) pH 10 on a bare IDE (i.e., without SMel coating).

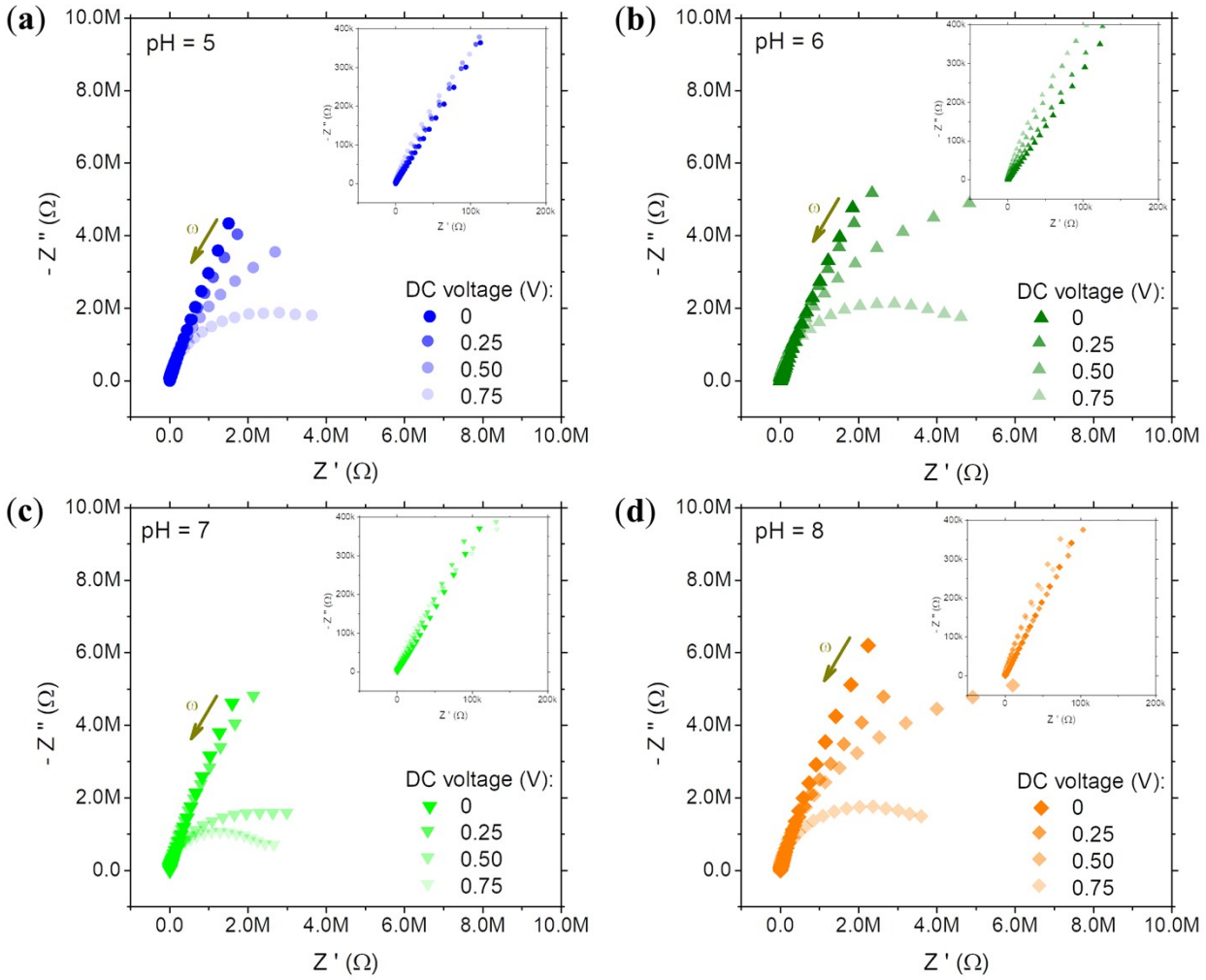

Figure S4. Nyquist plots of a SMel film applying a DC voltage between 0 and 0.75 V at different pH: (a) pH 5, (b) pH 6, (c) pH 7, and (d) pH 8.

Table S3: Fitting parameters at zero DC voltage of the different PBS solutions.

PBS	R_1 (Ω)	R_2 (10^7 Ω)	Q (10^{-7} Ω^{-1})	η (unitless)	χ^2
pH 2	460.80	5.10	0.25	0.82	0.003
pH 5	264.80	36.90	3.75	0.88	0.009
pH 6	278.00	1.36×10^{12}	3.69	0.89	0.020
pH 7	249.90	7.43	2.46	0.91	0.009
pH 8	378.10	14.86	4.18	0.90	0.018
pH 10	278.1	2.98	2.39	0.92	0.047

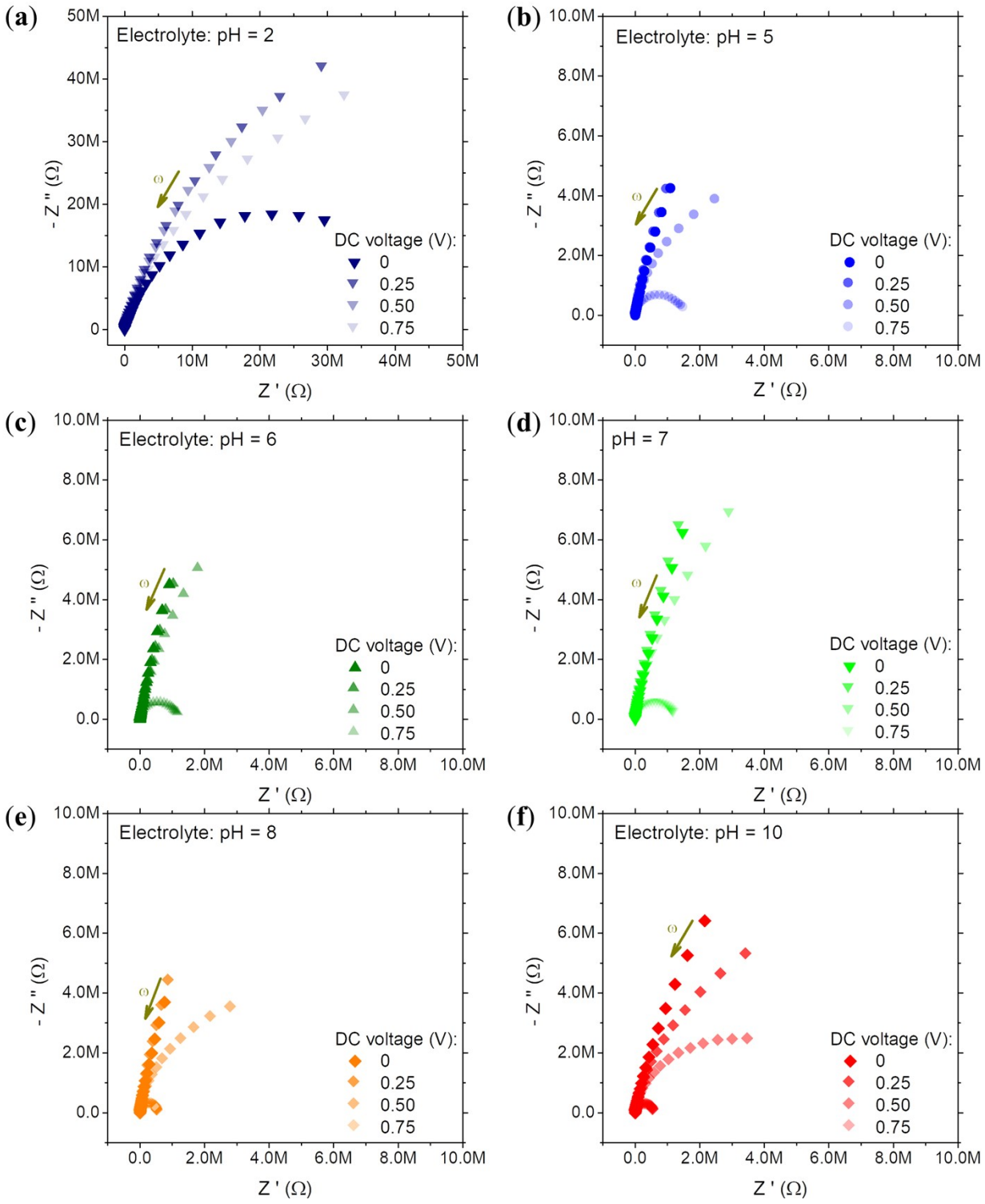

Figure S5. Nyquist plot of PBS electrolyte applying a DC voltage between 0 and 0.75 V at different pH: (a) pH 2, (b) pH 5, (c) pH 6, (d) pH 7, (e) pH 8, and (f) pH 10 on a bare IDE.

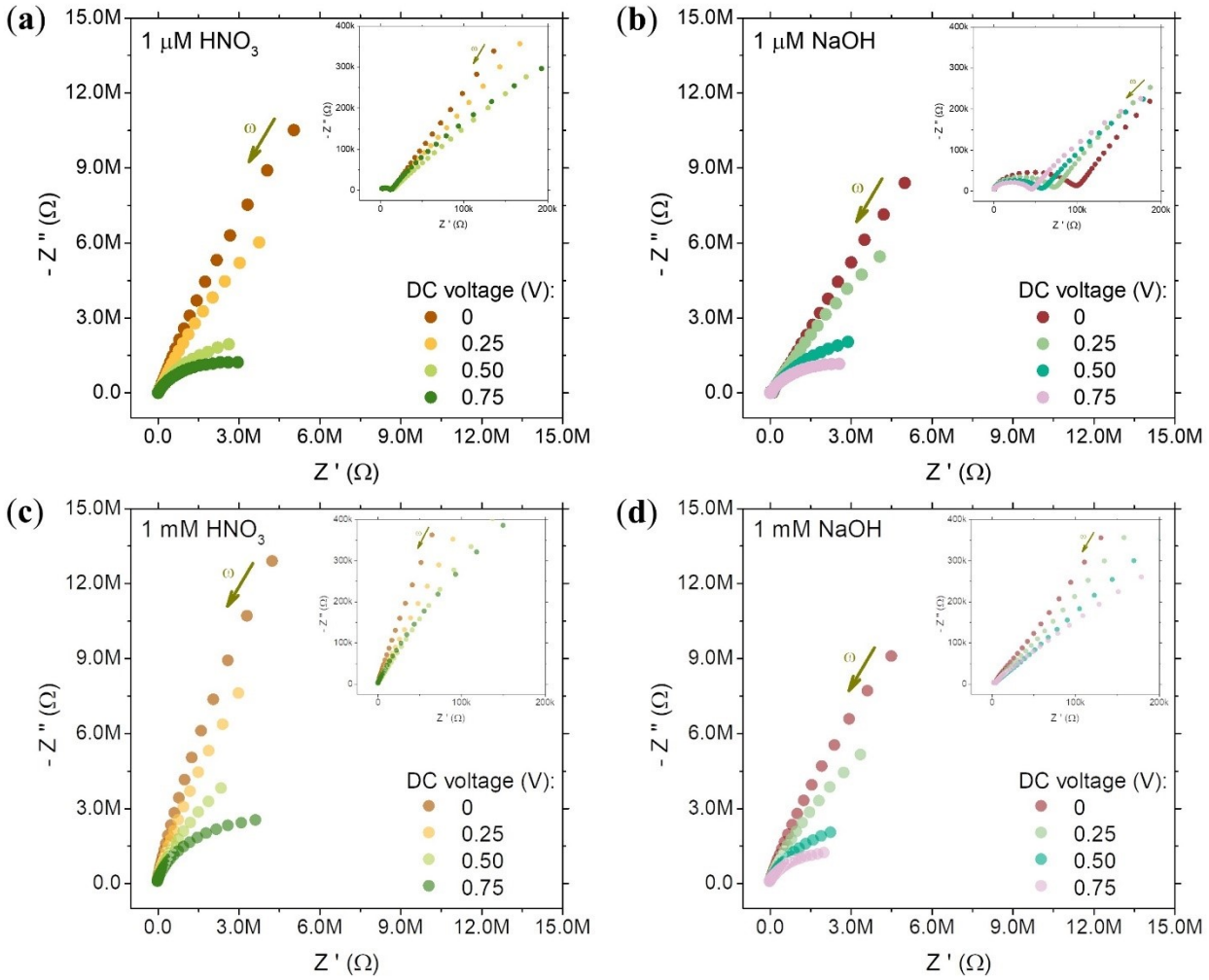

Figure S6. Nyquist plots of a SMel film applying a DC voltage between 0 and 0.75 V at different concentrations of (a, c) nitric acid and (b, d) sodium hydroxide (see legend).

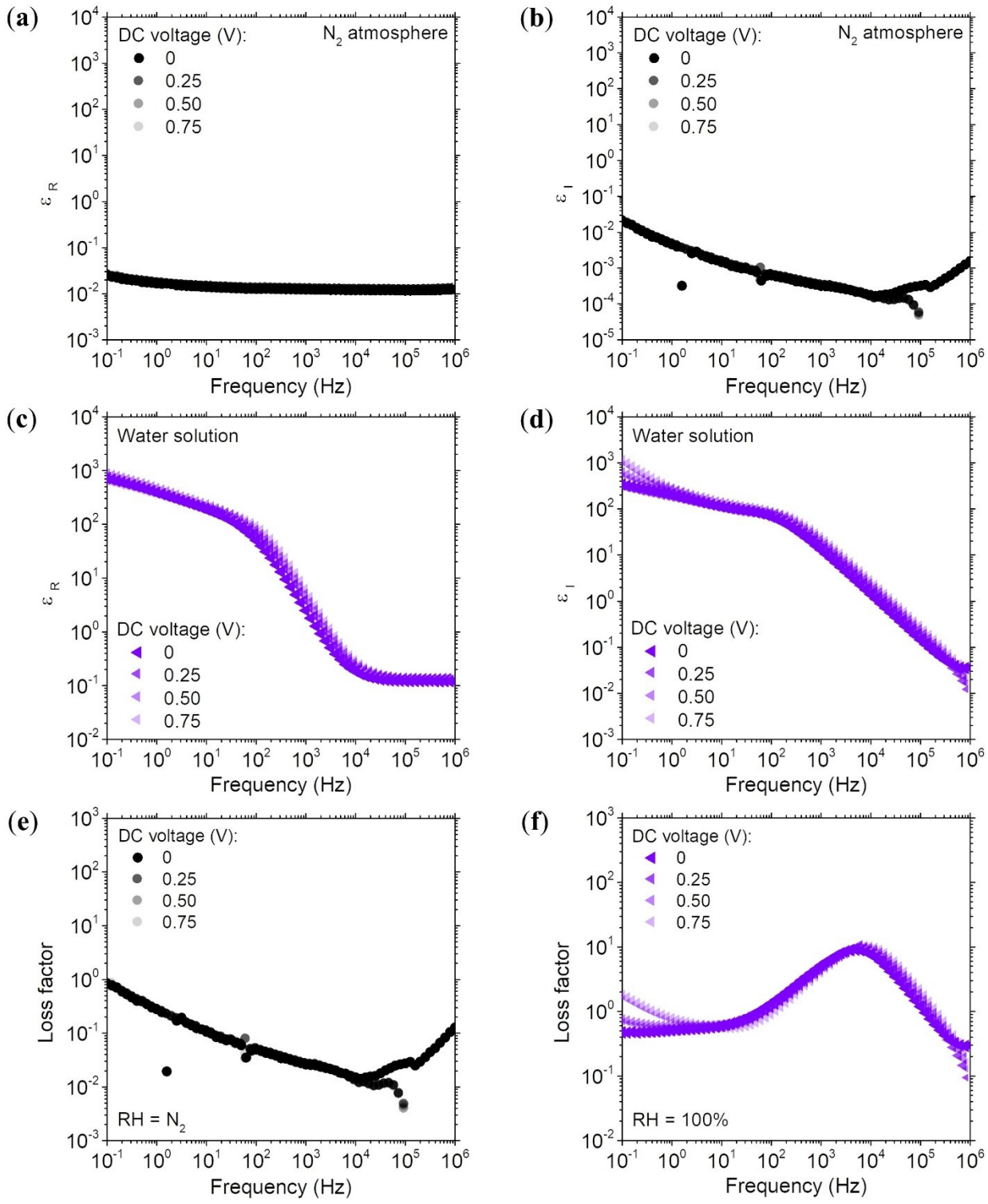

Figure S7. The (a, c) real and (b, d) imaginary parts of the dielectric permittivity and (e, f) Loss factor calculated from the impedance data of the SMel film applying a DC voltage between 0 and 0.75 V at different humidity levels: (a, c, e) N_2 atmosphere and (b, d, f) water solution.

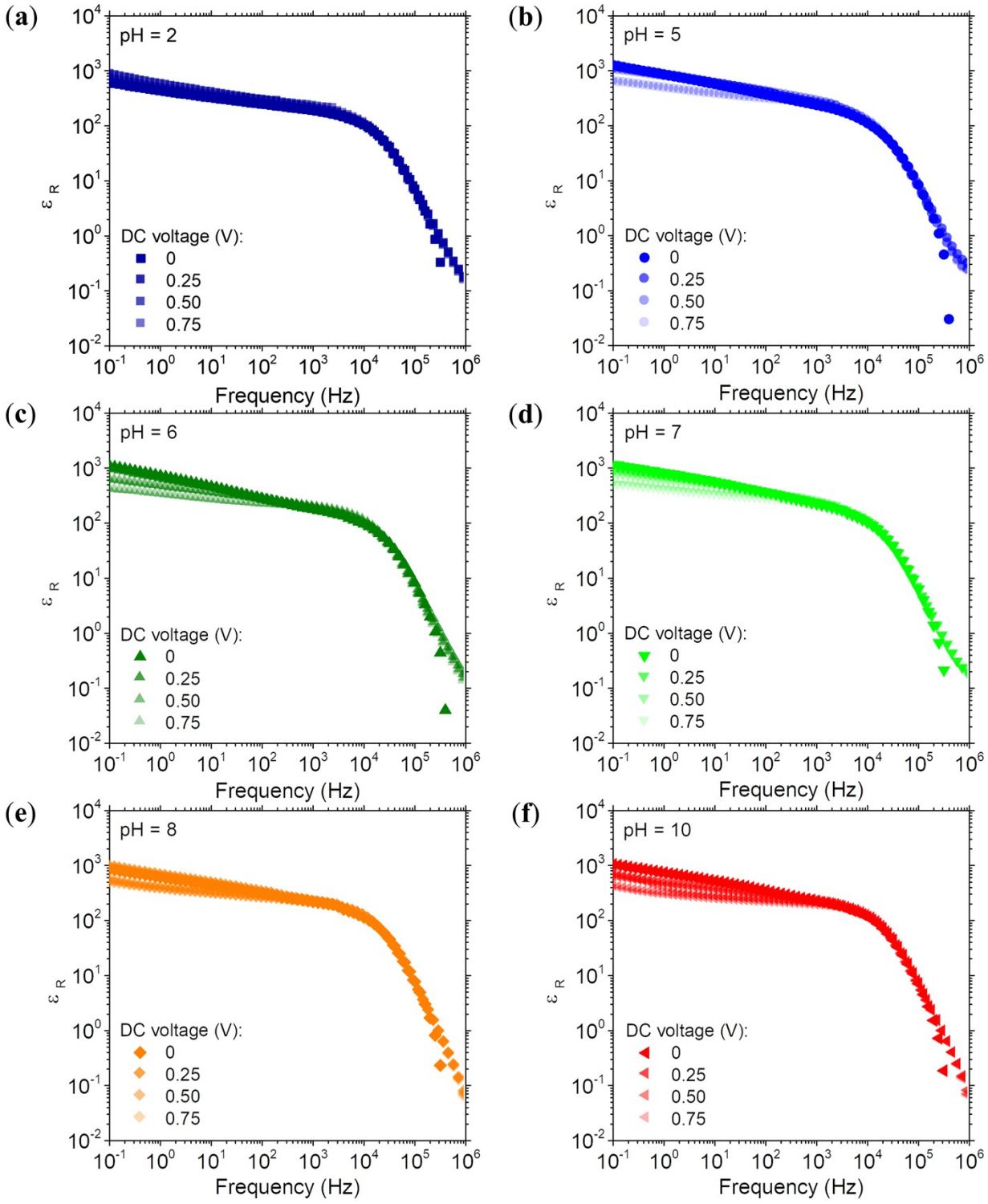

Figure S8. The real part of the dielectric permittivity calculated from the impedance data of the SMel film applying a DC voltage between 0 and 0.75 V at different pH: (a) pH 2, (b) pH 5, (c) pH 6, (d) pH 7, (e) pH 8, and (f) pH 10.

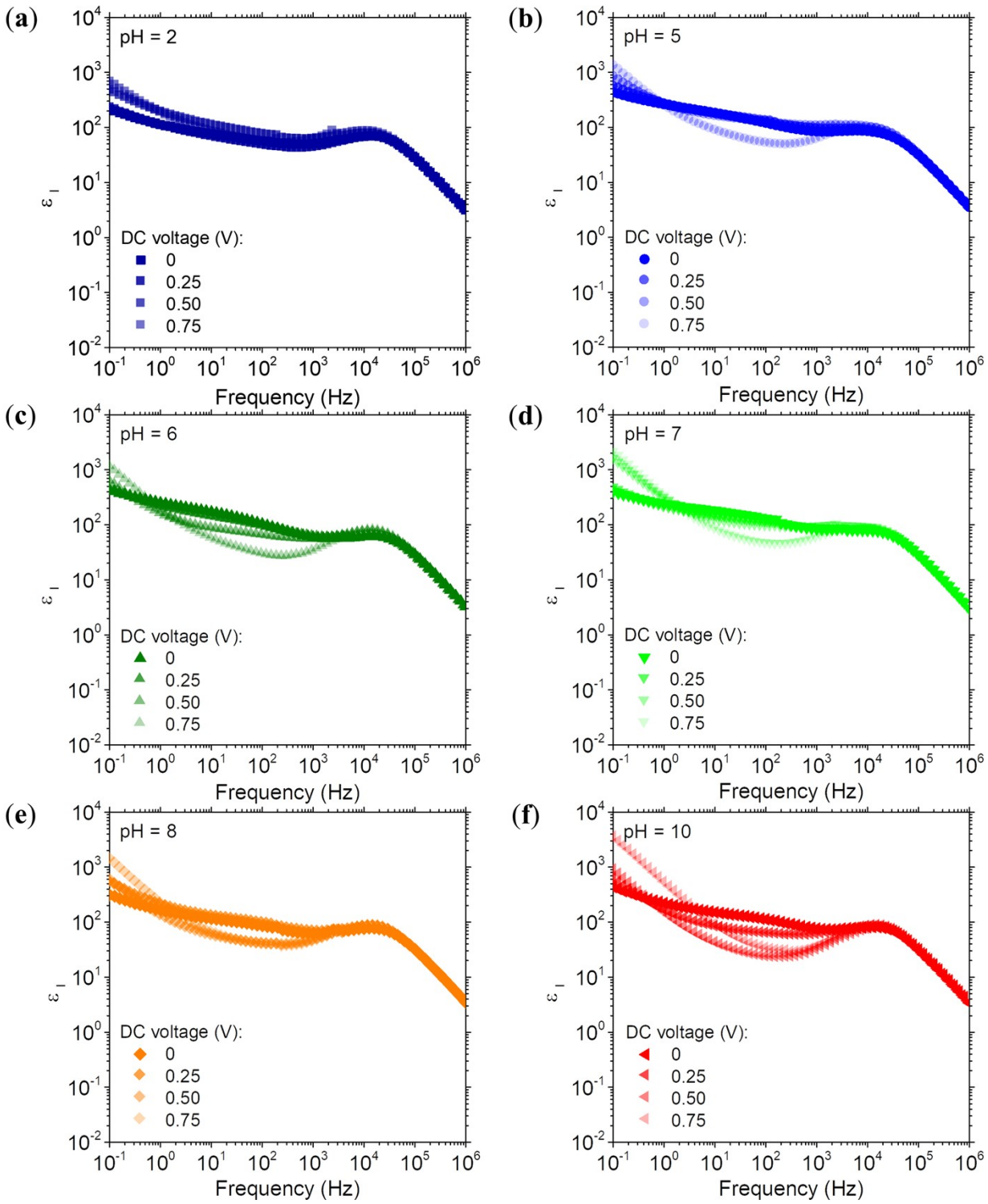

Figure S9. The imaginary part of the dielectric permittivity calculated from the impedance data of the SMel film applying a DC voltage between 0 and 0.75 V at different pH: (a) pH 2, (b) pH 5, (c) pH 6, (d) pH 7, (e) pH 8, and (f) pH 10.

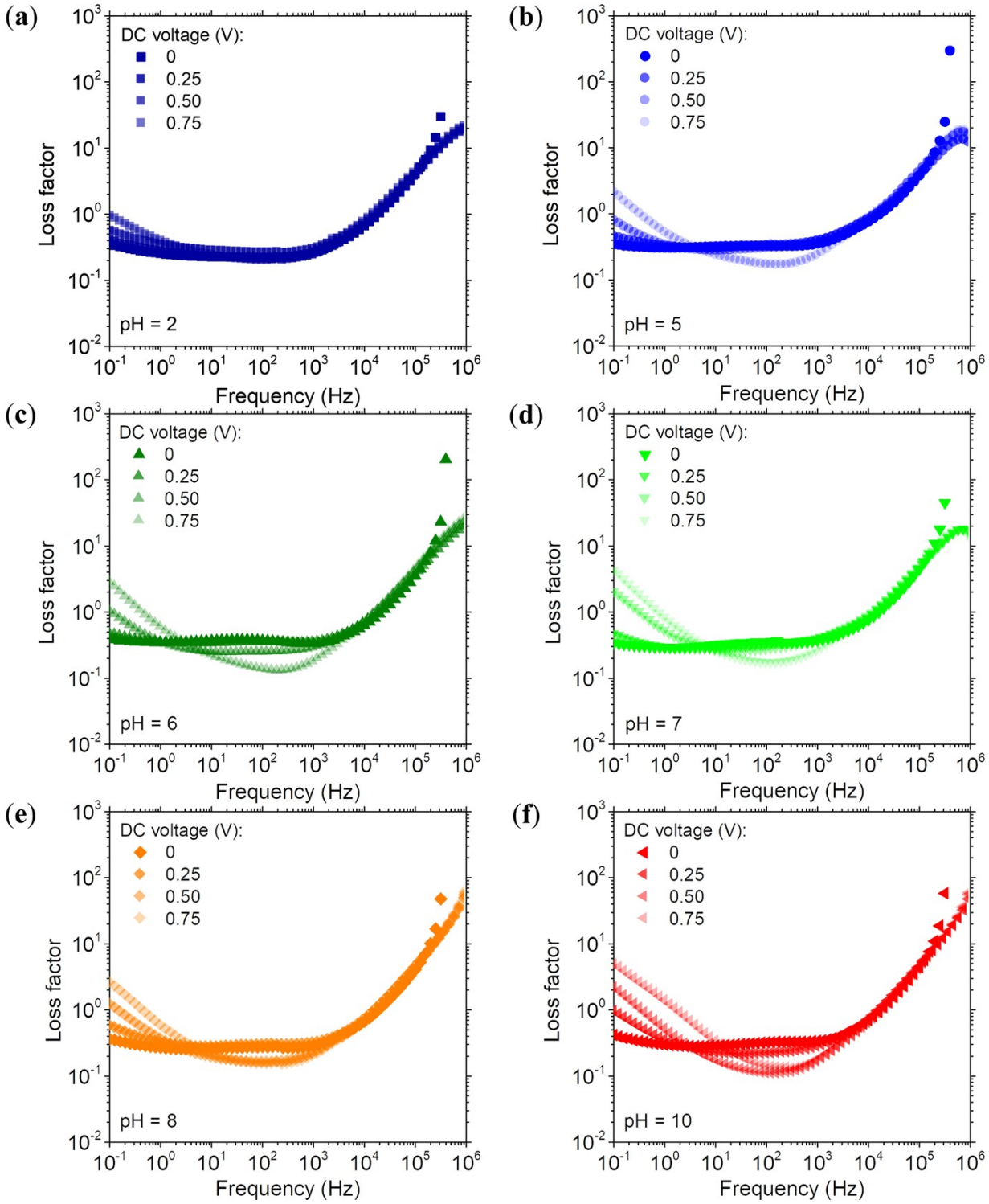

Figure S10. The loss factor of the SMel film applying a DC voltage between 0 and 0.75 V at different pH: (a) pH 2, (b) pH 5, (c) pH 6, (d) pH 7, (e) pH 8, and (f) pH 10.

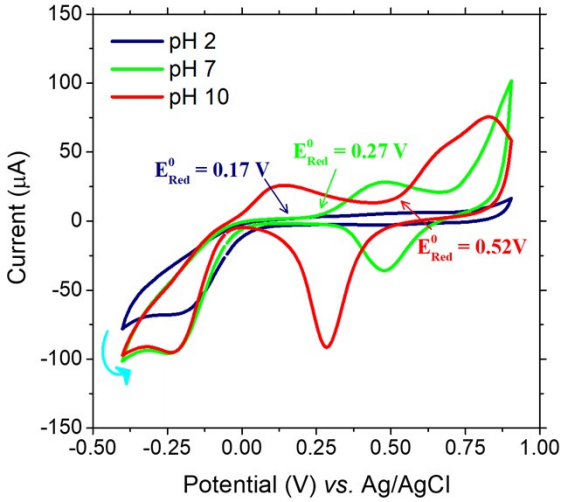

Figure S11. Cyclic voltammograms of SMel on gold as a working electrode using PBS electrolytes at pH 2, pH 7, and pH 10. Highlighted are the estimated reduction potentials.

B) Theoretical data analysis.

Density functional theory (DFT) calculations:

The design of oligomeric structures is based on Figure 1b in the main text (with $R_2 = R_3 = R_4 = H$). Figure S12 shows the cyclic oligomeric systems:

a) Mel_1: $2^{(1)}$-$5^{(2)}/2^{(2)}$-$8^{(3)}/2^{(3)}$-$8^{(4)}/2^{(4)}$-$8^{(1)}$

b) Mel_2: $2^{(1)}$-$5^{(2)}/2^{(2)}$-$8^{(3)}/2^{(3)}$-$5^{(4)}/2^{(4)}$-$8^{(1)}$

c) Mel_3: $2^{(1)}$-$8^{(2)}/2^{(2)}$-$5^{(3)}/2^{(3)}$-$5^{(4)}/2^{(4)}$-$5^{(1)}$

d) Mel_4: $2^{(1)}$-$5^{(2)}/2^{(2)}$-$5^{(3)}/2^{(3)}$-$5^{(4)}/2^{(4)}$-$5^{(1)}$

where $X^{(a)}$-$Y^{(b)}$ represents which units *a* and *b* are connected via a chemical bond between atoms X and Y (according to Figure 1b).

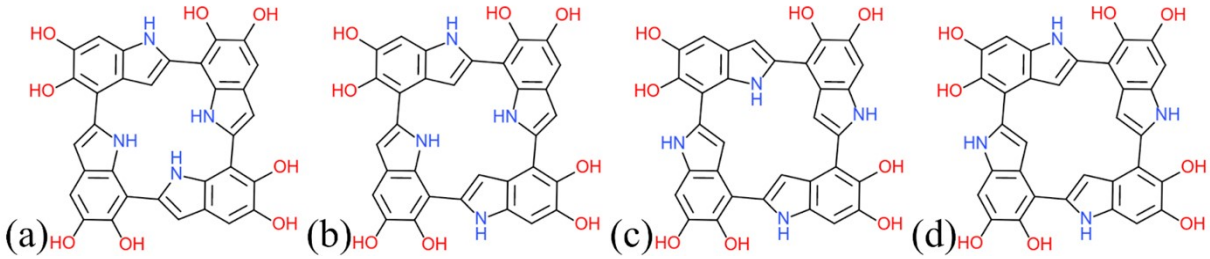

Figure S12. Oligomeric structures evaluated: a) Mel_1, b) Mel_2, c) Mel_3 and d) Mel_4.

The structures were designed with the aid of the Molden computational package[S1] and fully optimized in the framework of the density functional theory (DFT), considering B3LYP exchange-correlation hybrid functional and 6-311G(d,p) basis set on all the atoms.

The local reactivities on the oligomer structures were evaluated with the aid of condensed-to-atoms Fukui indices (CAFI)[S2] and molecular electrostatic potential (MEP) maps, Figure S12. CAFIs allow the identification of molecular sites that are prone to interact with nucleophilic (f_k^+) or electrophilic (f_k^+) external agents, being expressed by:

$$f_k^- = p_k(N) - p_k(N-1) \qquad (S1)$$

$$f_k^+ = p_k(N+1) - p_k(N) \qquad (S2)$$

where $p_k(N+1)$, $p_k(N)$, and $p_k(N-1)$ represent the electronic populations on the k-th atom of the structure (Mel) considering its anionic (Mel^{-1}, with N+1 electrons), neutral (Mel^0, with N electrons) and cationic (Mel^{+1}, with N-1 electrons) configurations. The electron populations on the atoms were estimated using the Hirshfeld charge partition method to avoid negative CAFI values.[S3,S4] MEPs were estimated via Chelp scheme.[S5] Color maps were designed with the Jmol computational package[S6] (CAFI) in combination with specifically developed Fortran 90 routines and the Gabedit computational package.[S7]

Aiming to identify the influence of external ions on the electronic structure of these oligomers, H^+ Na^+, OH^-, and NO_3^- species were placed around the most reactive sites (identified via CAFI and MEP). The structures were then re-optimized and evaluated at the same level of theory (DFT/B3LYP/6-311G(d,p)).

DFT discussion:

Figure S13 summarizes the CAFIs and MEPs obtained for melanin oligomers. Red and blue sites in CAFI (MEP) maps represent respectively reactive (negatively charged) and non-reactive (positively charged) sites. In general, sites with higher values of f^+ and f^- (red sites) represent regions that are prone to interact with nucleophiles (receiving electrons) and electrophiles (losing electrons). Note that the oligomers' reactivity centers on 3, 5, and 8 carbons (polymerization sites) and oxygens atoms.

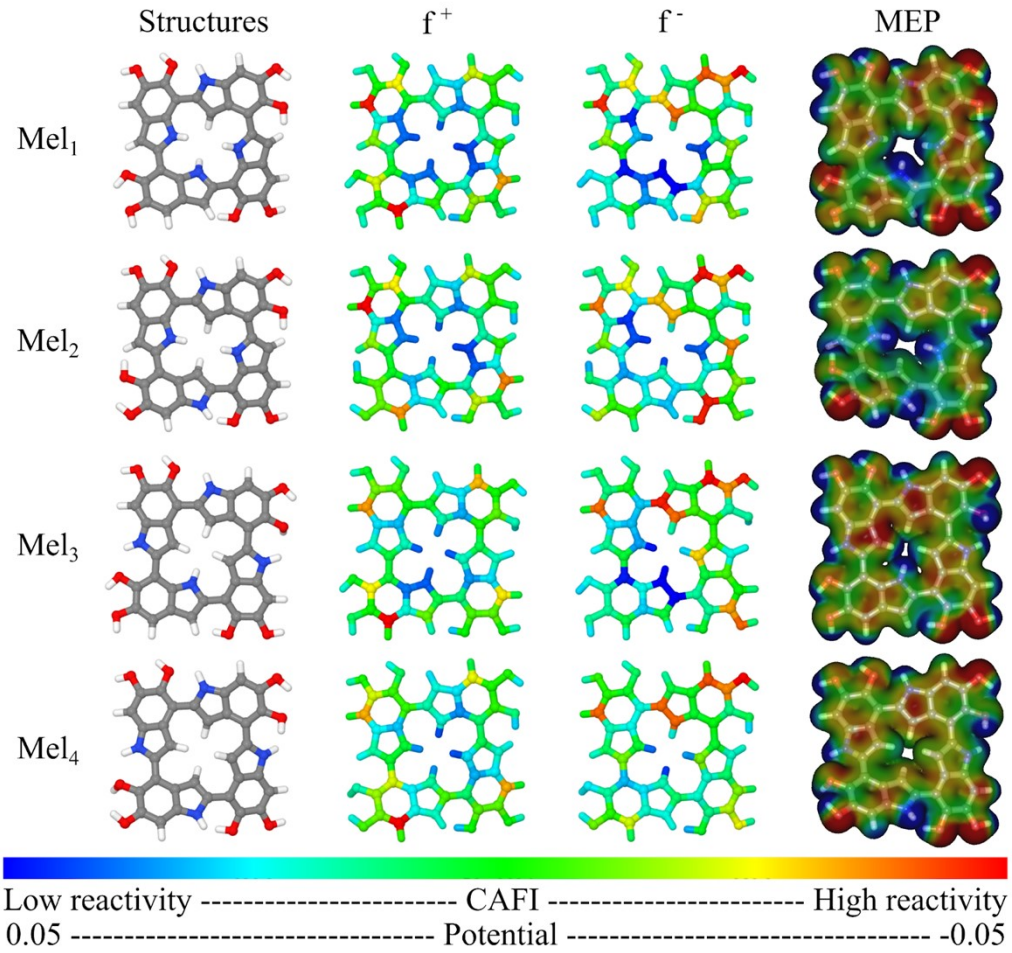

Figure S13. CAFI and MEP color maps of NF-eumelanin oligomers.

Figure S14 summarizes the distribution of electronic energy levels (KS orbitals) of isolated (neutral) melanin oligomers (Mel_k^0) about adsorbed systems: Mel_k^0/H^+, Mel_k^0/Na^+, Mel_k^0/OH^- and Mel_k^0/NO_3^-. Chemical changes are noticed for systems exposed to H^+ and OH^-. In these cases, it is noticed the attachment of H^+ at sites 3 (carbon) and 1 (nitrogen) and abstraction of an H atom from the nitrogen (site 1) of the Mel_k blocks promoted by HO^-. No such degradation effects are noticed for Na^+ and NO_3^- -based systems. In general, ions around NF-eumelanin blocks can significantly impact the position of electronic levels frontier. In particular, the shift of energy levels and the formation of new electronic levels inside the band gap of the isolated system suggest the existence of effective electrochemical doping processes in the eumelanin.

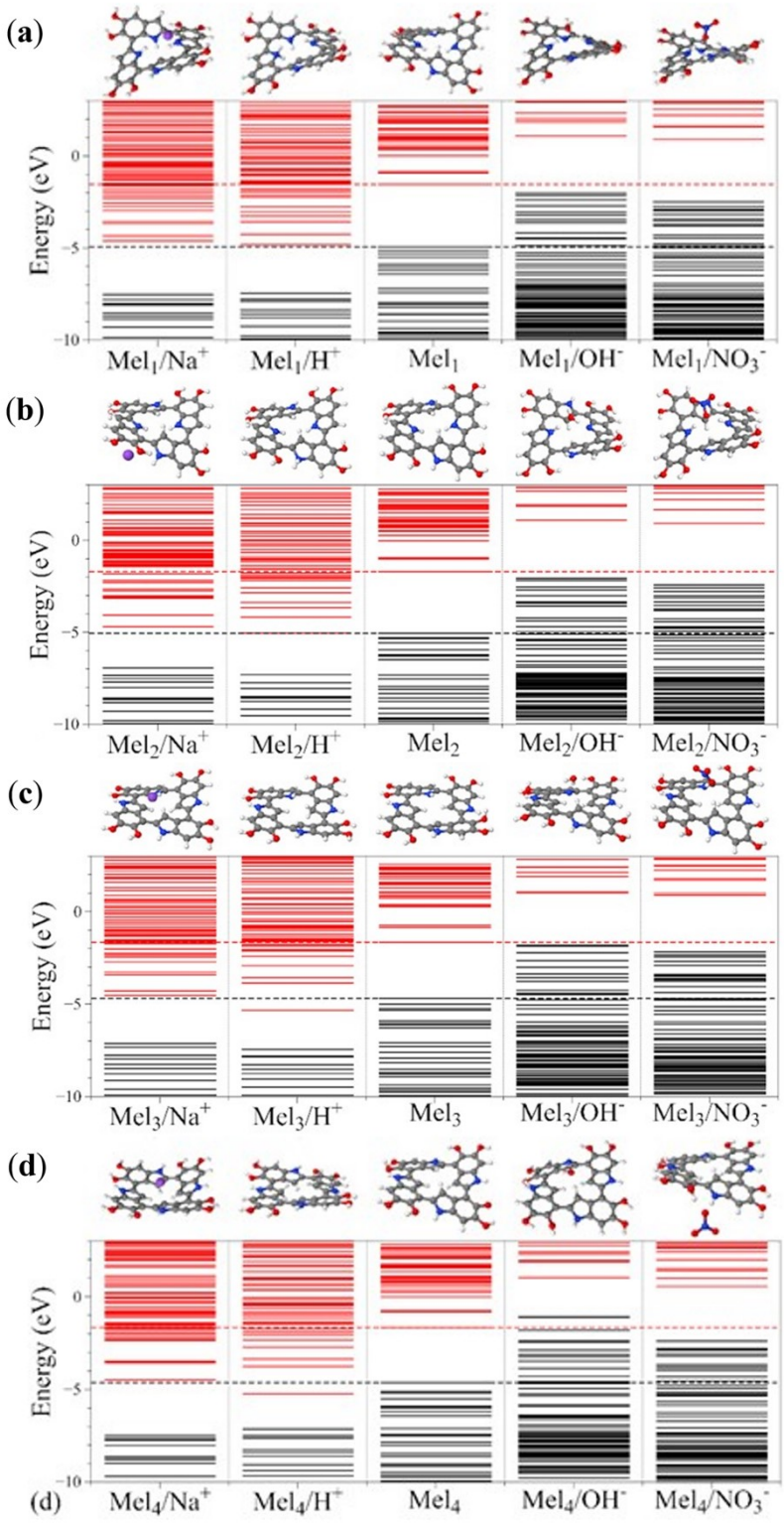

Figure S14. Influence of ions on the electronic levels of eumelanin oligomers: a) Mel_1, b) Mel_2, c) Mel_3, and d) Mel_4. Isolated Mel_k (center) and adsorbed systems cations (H^+ and Na^+ - left) and anions (OH^- and NO_3^- - right).

References

[S1] G. Schaftenaar, J. H. Noordik, *J. Comput. Aided. Mol. Des.* **2000**, *14*, 123.

[S2] W. Yang, W. J. Mortier, *J. Am. Chem. Soc.* **1986**, *108*, 5708.

[S3] R. K. Roy, K. Hirao, S. Pal, *J. Chem. Phys.* **1999**, *110*, 8236.

[S4] F. De Proft, C. Van Alsenoy, A. Peeters, W. Langenaeker, P. Geerlings, *J. Comput. Chem.* **2002**, *23*, 1198.

[S5] L. E. Chirlian, M. M. Francl, *J. Comput. Chem.* **1987**, *8*, 894.

[S6] nd, "Jmol: an open-source Java viewer for chemical structures in 3D. http://www.jmol.org/," **n.d.**

[S7] A.-R. Allouche, *J. Comput. Chem.* **2011**, *32*, 174.